

Citation for published version:

Zhang, Y, Bao, Y, Zhang, D & Bowen, CR 2015, 'Porous PZT ceramics with aligned pore channels for energy harvesting applications', *Journal of the American Ceramic Society*, vol. 98, no. 10, pp. 2980-2983.
<https://doi.org/10.1111/jace.13797>

DOI:

[10.1111/jace.13797](https://doi.org/10.1111/jace.13797)

Publication date:

2015

Document Version

Early version, also known as pre-print

[Link to publication](#)

This is the peer reviewed version of the following article: Zhang, Y, Bao, Y, Zhang, D & Bowen, CR 2015, 'Porous PZT ceramics with aligned pore channels for energy harvesting applications' *Journal of the American Ceramic Society*, which has been published in final form at [10.1111/jace.13797](https://doi.org/10.1111/jace.13797). This article may be used for non-commercial purposes in accordance with Wiley Terms and Conditions for Self-Archiving.

University of Bath

Alternative formats

If you require this document in an alternative format, please contact:
openaccess@bath.ac.uk

General rights

Copyright and moral rights for the publications made accessible in the public portal are retained by the authors and/or other copyright owners and it is a condition of accessing publications that users recognise and abide by the legal requirements associated with these rights.

Take down policy

If you believe that this document breaches copyright please contact us providing details, and we will remove access to the work immediately and investigate your claim.

Porous PZT ceramics with aligned pore channels for energy harvesting applications

Yan Zhang¹, Yinxiang Bao², Dou Zhang^{2,*}, and Chris R. Bowen³

¹Modern Engineering Training Center, Hunan University, Changsha 410083, China

²State Key Laboratory of Powder Metallurgy, Central South University, Changsha 410083, China

³Materials Research Centre, Department of Mechanical Engineering, University of Bath,

Claverton Down Road, BA2 7AY, UK

Abstract: In this paper aligned porous lead zirconate titanate (PZT) ceramics with high pyroelectric figures of merit were successfully manufactured by freeze casting using water-based suspensions. The introduction of aligned pores was demonstrated to have a strong influence on the resultant porous ceramics, in terms of mechanical, dielectric and pyroelectric properties. As the level of porosity was increased, the relative permittivity, dielectric loss and pyroelectric coefficient decreased while the Curie temperature increased. The aligned porous structure exhibited improvement in the compressive strength ranging from 19 to 35 MPa, leading to easier handling, better processability and wider applications for such type of porous material. Since the relative permittivity decreased to a larger extent than the pyroelectric coefficient with increasing porosity, both types of pyroelectric harvesting figures-of-merit (F_E and F_E') of the PZT ceramics with a porosity level of 25-45 vol.% increased from 11.41 to 12.43 $\text{pJm}^{-3}\text{K}^{-2}$ and 1.94 to 6.57 pm^3J^{-1} respectively, which were shown to be higher than the dense PZT counterpart.

I. Introduction

Pyroelectric energy conversion is of interest since it offers a novel way to convert waste heat into electricity by alternatively heating and cooling a pyroelectric material.¹⁻³ This approach has attracted much interest in areas such as powering low-power electronics and battery-less wireless sensors. For pyroelectric energy harvesting applications, the main requirements are high pyroelectric coefficient, high figures of merit and low permittivity. An energy harvesting figure of merit, F_E shown in Eqn. 1, has been widely used for materials selection and materials design for pyroelectric harvesting applications.⁴⁻⁶

$$F_E = \frac{p^2}{\epsilon_{33}^T} \quad \text{Eqn. 1}$$

where p is the pyroelectric coefficient and ϵ_{33}^T is the permittivity of the pyroelectric material at constant stress. Efforts to improve the performance of ferroelectric ceramics for a variety of applications often focus on dense materials via chemical modification (doping, substitution)^{7, 8} or the employment of the single crystals.^{9, 10} Due to the complexity of developing new formulations and the high cost, low Curie temperature and poor mechanical properties of single crystals, the applications of pyroelectric harvesting materials are limited. From Eqn. 1, a porous structure with decreased permittivity has the potential to provide benefits for energy harvesting applications if the pyroelectric coefficient is not reduced significantly. Lang et al. observed an improvement in both the piezoelectric and pyroelectric figures of merit in porous lead zirconate titanate (PZT) prepared by burning out the organic particles as a result of the significantly reduced relative permittivity of porous structures with 3-0 and 3-3 connectivities.

The introduction of porosity also has the potential to decrease the heat capacity which leads to an improvement of the thermal response; however, porosity can also decrease the electrical resistivity and pyroelectric coefficient.⁴ This complex relationship between pyroelectric, dielectric and thermal properties means that there is potential of tuning the porosity to achieve the optimum response for a given application.

Owing to many levels of hierarchical structures from macroscopic to microscopic length scales of the microstructure, directional freezing process has recently attracted interest in the fabrication of porous ceramic with lamellar oriented architectures. By taking advantage of the principle of unidirectional solidification of a liquid vehicle, such as water, freeze casting, also called ice templating,^{12, 13} has been developed as a simple and novel method with low production cost for the preparation of oriented porous structures. In this paper, porous PZT ceramics were achieved by freeze casting, and their microstructural, relative permittivity, dielectric loss, pyroelectric and mechanical properties were investigated and compared.

II. Experimental Procedure

Lead zirconate titanate (PZT) powder (PZT5-A; Baoding Hengsheng Acoustics Electron Apparatus Co. Ltd., Baoding, China) with a mean particle size of 0.25 μm , deionized water, polyvinyl alcohol (PVA, 420, Kuraray Co. Ltd, Japan) and ammonium polyacrylate (HydroDisper A160, Shenzhen Highrun Chemical Industry Co. Ltd, P. R. China) were used as the starting materials, freezing vehicle, the binder and the dispersant, respectively. PZT suspensions were ball-milled for 24 h in zirconia media and de-aired by stirring in a vacuum desiccator, until complete removal of air bubbles. The freezing process, pore characterization

methodology and mechanical measurements were given in details in previous works.^{14, 15}

Conventional ceramic processing technique was employed to prepare the dense ceramic for comparison with the freeze-cast porous materials. Burning out the organic particles was utilized to prepare the conventional porous ceramic for the mechanical comparison with the freeze-cast porous materials. Burnout of the PVA binder was carried out at 500 °C for 1 h with a heating rate of 1 °C/min. Final sintering was carried out at 1200 °C with a heating rate of 5 °C/min under a PbO-rich atmosphere to minimize the lead (Pb) loss during sintering, followed by natural cooling to room temperature. Before electrical properties measurement, corona poling was conducted on the sintered dense and porous samples at 120 °C by applying an electric field of 30 kV for 30 min, and the material was aged for 24 h prior to testing. The relative permittivity and dielectric loss of the porous ceramics were measured by an impedance analyzer (Agilent-4294A, Agilent Technologies Inc.) at 1 kHz from 293-673 K. The pyroelectric coefficient was determined by the Byer-Roundy method and derived from the equation 2:¹⁶

$$I = pA\left(\frac{dT}{dt}\right) \quad \text{Eqn. 2}$$

where I is the pyroelectric current, p is the pyroelectric coefficient, A is the area of capacitor and dT/dt is the rate of change of temperature. The pyroelectric current I was measured using an electrometer (Model 6517A, Keithley, USA) at the temperature 300 K.

III. Results and discussion

Fig. 1 (a)-(d) show scanning electron microscopy (SEM) micrographs of dense and porous PZT ceramics with porosities of 3 vol.%, 25 vol.%, 35 vol.% and 45 vol.%, respectively. The

dense PZT ceramic exhibited a similar grain size of 0.8-1.3 μm to the porous counterparts, as shown in Fig. 1(a). All the porous ceramics prepared by freeze casting exhibited a well aligned 2-2 type PZT-air laminate composite connectivity as shown in Fig. 1(b)-(d). As the level of porosity increased from 25% to 45%, the lamellar oriented pore width decreased from 22-30 to 3-8 μm and the lamellar thickness increased from 5-9 to 28-32 μm . According to our previous work,^{13, 17, 18} adjustments in the lamellar pore width from 1 to 60 μm , the lamellar thickness from 1 to 40 μm and the second circular pore from 6 to 400 μm can be achieved by tailoring the particle sizes of the powders, solid loading of the suspension, the organic additions and the freezing conditions. The volume specific heat capacity c_E of the dense and porous PZT ceramics with porosities of 3 vol.%, 25 vol.%, 35 vol.% and 45 vol.% were 2.43, 1.88, 1.63 and 1.38 $\text{MJ}\cdot\text{m}^{-3}\cdot\text{K}^{-1}$ respectively, which were calculated by the following equation 3:

$$c_E = 2.5(\text{MJ} \cdot \text{m}^{-3} \cdot \text{K}^{-1})(1 - \varphi) \quad \text{Eqn. 3}$$

where φ is the porosity of the PZT ceramic and $2.5 \text{ MJ}\cdot\text{m}^{-3}\cdot\text{K}^{-1}$ is the c_E of the dense material.

Fig. 2 (a) and (b) show the influence of temperature ranging from 20 to 400 $^{\circ}\text{C}$ and porosity ranging from 3 to 45 vol.% on the relative permittivity (ϵ_{33}^T) and dielectric loss ($\tan \delta$) of dense and porous PZT ceramics at a frequency of 1k Hz, respectively. The relative permittivity decreased as the porosity increased at any temperature and the peak of maximum ϵ_{33}^T decreased with increasing porosities, as shown in Fig. 2 (a). It can be found that Curie temperature (T_C) of dense PZT ceramics (203 $^{\circ}\text{C}$) shifts to higher temperature (210-229 $^{\circ}\text{C}$)

with an increase of porosity. The introduction of air, in the form of porosity, that possesses a lower permittivity than PZT, and the decreased internal stress in the porous samples¹⁹ are thought to account for the decrease of relative permittivity and the increase of T_C (operating temperature), respectively. In addition, the relative permittivity was proportional to the porosity (P) at the range of temperatures studied. For porous PZT sample at 25 °C, the relationship can be fitted by equation 4:

$$\varepsilon_{33}^T = 1437 - 1953P \quad \text{Eqn. 4}$$

The reduced relative permittivity as a result of the introduction of porosity can lead to positive effects on the pyroelectric performance of porous PZT ceramics, such as F_E and F_E' , which will be discussed in the following section. Fig. 2 (b) shows that the dielectric loss increased with an increase of the porosity. This was mainly attributed to the pores, which introduced high dielectric loss in porous PZT ceramic. When the temperature is higher than 246 °C at porosity of 45 vol.%, the dielectric loss of the porous PZT ceramic increased sharply.

Fig. 3(a) shows the effects of porosity on the pyroelectric coefficient and compressive strength of porous PZT ceramics. As the level of porosity is increased, both the pyroelectric coefficient and compressive strength decreased from 316 to 269 $\mu\text{C}/\text{m}^2\text{K}$ and from 35 to 19 MPa, respectively, as shown in Fig. 3(a). The presence of highly aligned 2-2 type porosity (Fig. 1) as a result of the freeze casting method led to a slightly higher pyroelectric coefficient and lower permittivity than reported by Lang et al. for PZT with spherical pores that exhibit 3-0 or 3-3 connectivity,¹¹ e.g. 316 versus 222 $\mu\text{C}/\text{m}^2\text{K}$ for pyroelectric coefficient and 949 versus 1000 for relative permittivity at the porosity of 25 vol.%. The freeze-cast porous PZT

ceramics exhibited 250 % to 300 % higher in the compressive strength than that of porous samples prepared by the same conventional method which Lang et al used as shown in Fig. 3a, leading to easier handling, better processability and wider applications for such type of porous material. Previous work has indicated that, in addition to Eqn. 1, a modified figure of merit F_E' that includes the influence of volume heat capacity c_E can be used to select and compare materials for pyroelectric energy harvesting when the harvesting element is subjected to an incident power density,²⁰ as shown in equation 5:

$$F_E' = \frac{p^2}{\epsilon_{33} \cdot (c_E)^2} \quad \text{Eqn. 5}$$

Fig. 3(b) shows the effects of porosity on the figures-of-merit of F_E and F_E' of porous PZT ceramics. Both types of figures-of-merit (F_E and F_E') increased with an increase of porosity as seen from Fig. 3(b), e.g. 11.41 to 12.4e pJm⁻³K⁻² and 1.94 to 6.57 pm³J⁻¹, respectively.

Because a decrease in relative permittivity of PZT ceramics (Fig. 2a) was more than that in pyroelectric coefficient (Fig. 3a) with increasing porosity, the figure of merit (p^2/ϵ_{33}) still increased with the increase of porosity. Compared with the conventional sintered dense ceramic with 3 vol.% porosity, the material with porosity higher than 25 vol.% exhibited higher F_E and F_E' values, demonstrating that figures of merit can be enhanced by inducing porosity. Compressive strength, dielectric and pyroelectric properties of porous PZT ceramics can be readily tailored and applied in a range of pyroelectric harvesting applications. The ability to produce aligned porosity also provides opportunities to tailor heat transfer characteristics such as thermal conductivity and diffusivity.

IV. Conclusions

Porous PZT ceramics with aligned pore channels were readily fabricated using freeze casting at low cost, and characterized in terms of dielectric and pyroelectric properties. The lamellar oriented pore width decreased from 22-30 to 3-8 μm and the lamellar thickness increased from 5-9 to 28-32 μm with the increase of the porosity from 25 to 45 vol.%. The relative permittivity, pyroelectric coefficient and volume specific heat of the porous PZT decreased with the increase of the porosity. These changes led to the porous samples with more than 25 vol.% porosity possessing higher pyroelectric harvesting F_E and F_E' figures of merit compared to dense PZT. Further work is in progress to explore the influences of the aligned pore-size distribution, pore shape and pore combination on the pyroelectric properties of porous ceramics for energy harvesting applications.

Acknowledgments

This research was financially supported by Natural Science Foundation of China (Nos. 51072235 and 51172288), the Defense Industrial Technology Development Program (No. A1420133028), and the Fundamental Research Funds for Central Universities in Hunan University (No. 2014-041). Bowen acknowledges funding from the European Research Council under the European Union's Seventh Framework Programme (FP/2007-2013) / ERC Grant Agreement no. 320963 on Novel Energy Materials, Engineering Science and Integrated Systems (NEMESIS).

References

1. Y. L. Felix, J. Hwan Ryul, S. L. Christopher, and P. Laurent, "Pyroelectric energy conversion using PLZT ceramics and the ferroelectric-ergodic relaxor phase transition," *Smart Materials and Structures*, 22[2] 025038 (2013).
2. C. R. Bowen, J. Taylor, E. LeBoulbar, D. Zabek, A. Chauhan, and R. Vaish, "Pyroelectric materials and devices for energy harvesting applications," *Energy & Environmental Science*, 7 25-44 (2014).
3. W. Liu, G. Wang, S. Cao, C. Mao, C. Yao, F. Cao, and X. Dong, "Pyroelectric Properties of Highly Ordered $\text{Pb}(\text{Sc}_{0.5}\text{Ta}_{0.5})\text{O}_3$ Ceramics by a Two-Step Sintering Technique," *Journal of the American Ceramic Society*, 93[12] 4030-32 (2010).
4. A. Navid, C. S. Lynch, and L. Pilon, "Purified and porous poly(vinylidene fluoride-trifluoroethylene) thin films for pyroelectric infrared sensing and energy harvesting," *Smart Materials and Structures*, 19[5] 055006 (2010).
5. N. Ashcon and P. Laurent, "Pyroelectric energy harvesting using Olsen cycles in purified and porous poly(vinylidene fluoride-trifluoroethylene) [P(VDF-TrFE)] thin films," *Smart Materials and Structures*, 20[2] 025012 (2011).
6. R. V. K. Mangalam, J. C. Agar, A. R. Damodaran, J. Karthik, and L. W. Martin, "Improved pyroelectric figures of merit in compositionally graded $\text{PbZr}_{1-x}\text{Ti}_x\text{O}_3$ thin films," *ACS Applied Materials and Interfaces*, 5[24] 13235-41 (2013).

7. H. Zhang, S. Jiang, K. Kajiyoshi, and J. Xiao, "Dielectric, Ferroelectric, Pyroelectric, and Piezoelectric Properties of La-Modified Lead-Free Sodium–Potassium Bismuth Titanate Thick Films," *Journal of the American Ceramic Society*, 93[3] 750-57 (2010).
8. C. Wu, G. Cai, W. Luo, Q. Peng, X. Sun, and W. Zhang, "Enhancement of pyroelectric properties of composite thick films using Mn-doped PZT," *Sensors and Actuators A: Physical*, 199[0] 24-29 (2013).
9. R. Sun, J. Wang, F. Wang, T. Feng, Y. Li, Z. Chi, X. Zhao, and H. Luo, "Pyroelectric properties of Mn-doped $94.6\text{Na}_{0.5}\text{Bi}_{0.5}\text{TiO}_3$ - 5.4BaTiO_3 lead-free single crystals," *Journal of Applied Physics*, 115[7] 074101-01-4 (2014).
10. O. V. Malyshkina, V. S. Lisitsin, J. Dec, and T. Łukasiewicz, "Pyroelectric and dielectric properties of calcium barium niobate single crystals," *Phys. Solid State*, 56[9] 1824-27 (2014).
11. S. B. Lang and E. Ringgaard, "Measurements of the thermal, dielectric, piezoelectric, pyroelectric and elastic properties of porous PZT samples," pp. 739-42 in *Electrical Insulation and Dielectric Phenomena, 2009. CEIDP '09. IEEE Conference*.
12. E. Munch, M. E. Launey, D. H. Alsem, E. Saiz, A. P. Tomsia, and R. O. Ritchie, "Tough, Bio-Inspired Hybrid Materials," *Science*, 322[5907] 1516-20 (2008).
13. Y. Zhang, J. Zeng, D. Zhang and K. C. Zhou, "Control of pore structures and sizes in freeze cast ceramics," *Advances in Applied Ceramics* 112[7] 405-11 (2013).

14. Y. Zhang, K. C. Zhou, D. Zhang, X. Y. Zhang, Z. Y. Li, G. Liu, T. W. Button, "Porous hydroxyapatite ceramics fabricated by an ice-templating method," *Scripta Materialia*, 64[5] 426-29 (2011).
15. Y. Zhang, L. Chen, J. Zeng, K. Zhou, and D. Zhang, "Aligned porous barium titanate/hydroxyapatite composites with high piezoelectric coefficients for bone tissue engineering," *Materials Science and Engineering: C*, 39 143-49 (2014).
16. R. L. Byer, C. B. Roundy, "Pyroelectric coefficient direct measurement technique and application to a NSEC response time detector," *Ferroelectrics*, 3 333-38 (1972).
17. Y. Zhang, Y. X. Bao, D. Zhang, and K. C. Zhou, "Effects of rheological properties on ice-templated porous hydroxyapatite ceramics," *Materials Science and Engineering: C*, 33[11] 340-46 (2013).
18. D. Zhang, Y. Zhang, R. Xie, and K. Zhou, "Freeze gelcasting of aqueous alumina suspensions for porous ceramics," *Ceramics International*, 38[7] 6063-66 (2012).
19. G. Zhang, S. Jiang, Y. Zeng, Y. Zhang, Q. Zhang, and Y. Yu, "High Pyroelectric Properties of Porous $\text{Ba}_{0.67}\text{Sr}_{0.33}\text{TiO}_3$ for Uncooled Infrared Detectors," *Journal of the American Ceramic Society*, 92[12] 3132-34 (2009).
20. C. R. Bowen, J. Taylor, E. Le Boulbar, D. Zabek, V. Yu. Topolov, "A modified figure of merit for pyroelectric energy harvesting," *Materials Letters*, 138[2015] 243-46 (2015).

Figure caption

Fig. 1 SEM images of porous PZT ceramics with different porosities. The solidification direction was parallel to the page and the lamellar orientation. (a) dense with 3 vol.% porosity, (b) 25 vol.% porosity, (c) 35 vol.% porosity, and (d) 45 vol.% porosity.

Fig. 2 Relative permittivity (ϵ_{33}^T) and dielectric loss ($\tan \delta$) of dense and porous PZT ceramics as a function of temperature and porosity: (a) relative permittivity, inset is the relationship between relative permittivity of the freeze-cast PZT ceramics and porosity at 25°C, and (b) dielectric loss.

Fig. 3 Pyroelectric coefficient, compressive strength and figure-of-merit of dense and porous PZT ceramics as a function of porosity at 300 K and 1k Hz: (a) Compressive strength and pyroelectric coefficient, (b) figures-of-merit of F_E and F_E' .

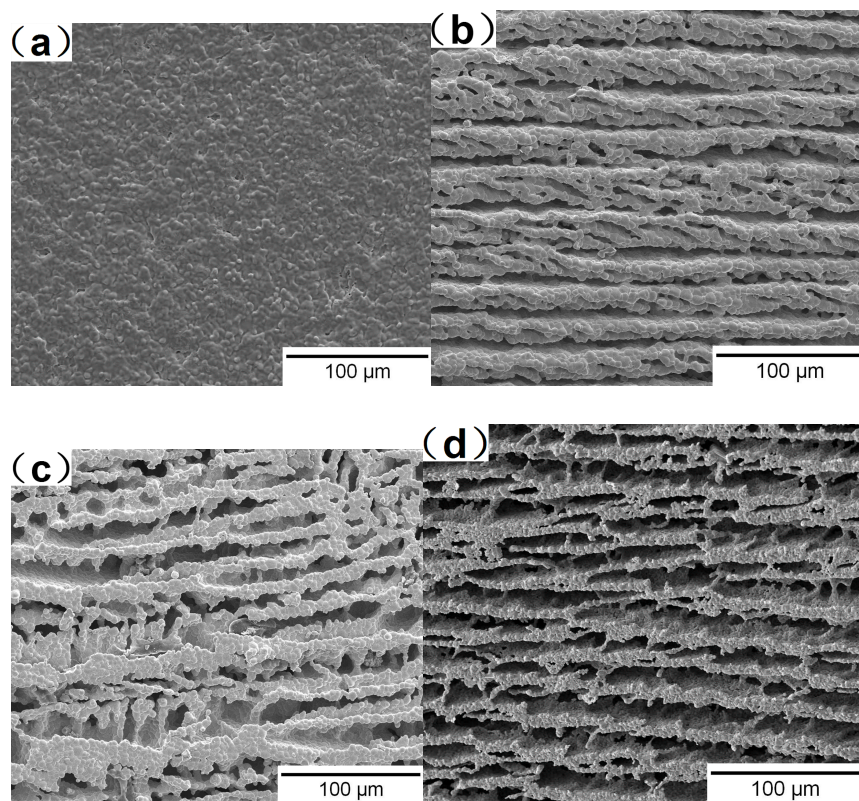


Figure 1

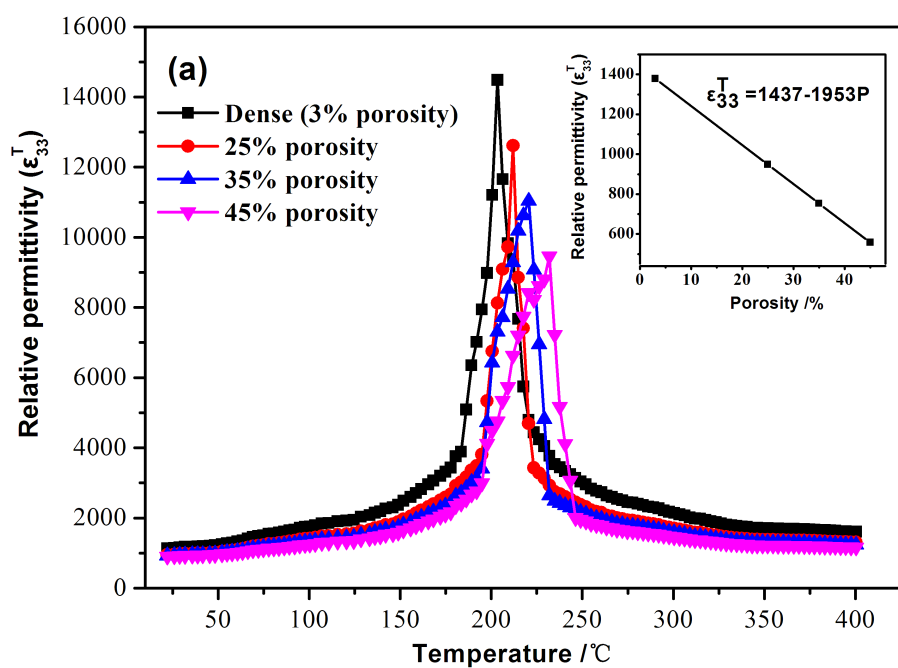
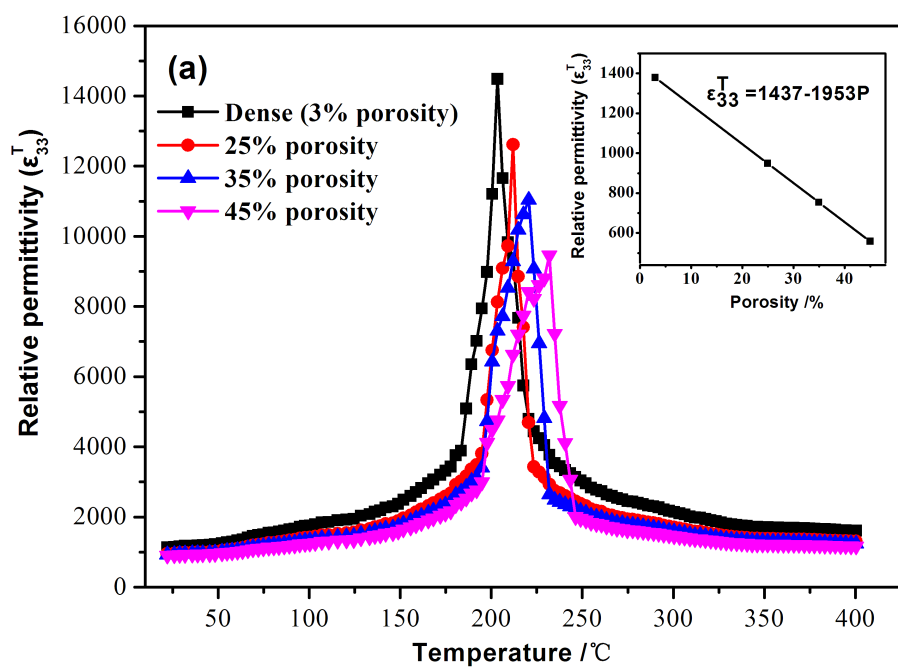


Figure 2

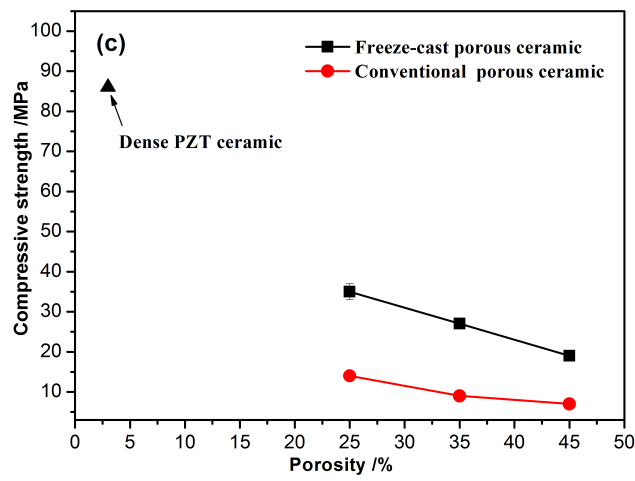
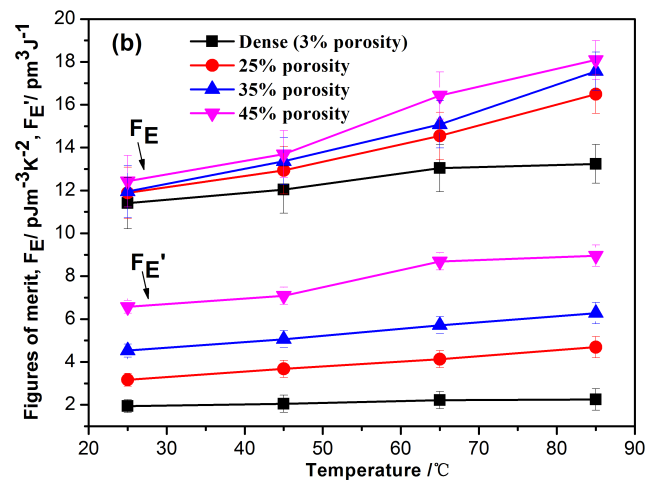
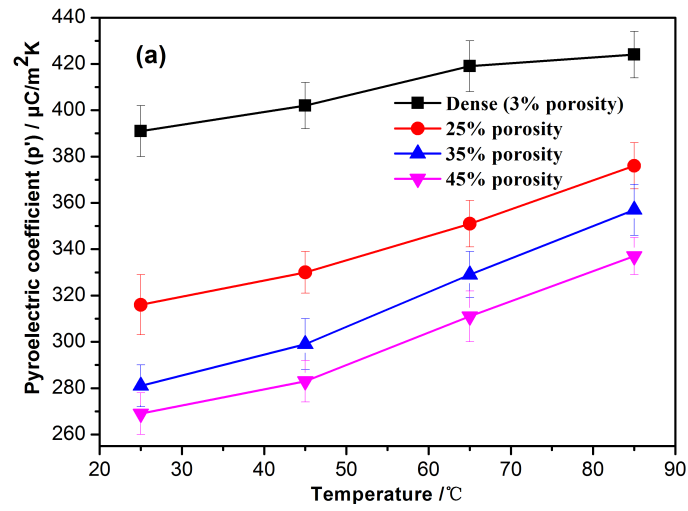


Figure 3